

Moisture content assessment of dried Hami jujube using image colour analysis

BENXUE MA^{1,2*}, CONG LI¹, YUJIE LI¹, WENXIA WANG¹, GUOWEI YU¹,
WANCHENG DONG¹, YUANJIA ZHANG¹

¹College of Mechanical and Electrical Engineering, Shihezi University, Shihezi, P.R. China

²Key Laboratory of Northwest Agricultural Equipment, Ministry of Agriculture and Rural Affairs, Shihezi, P.R. China

*Corresponding author: mbx_shz@163.com

Citation: Ma B.X., Li C., Li Y.J., Wang W.X., Yu G.W., Dong W.C., Zhang Y.J. (2022): Moisture content assessment of dried Hami jujube using image colour analysis. Czech J. Food Sci., 40: 33–41.

Abstract: To investigate the feasibility of image colour information in predicting the moisture content of dried Hami jujube, the images were obtained under different colour space models, and the colour model component mean and chromaticity frequency sequences of R, G, B, H, S, V, L^* , a^* and b^* were extracted through image analysis. After optimising the colour model component mean and chromaticity frequency sequence, the model was established and compared. The results showed that the GA-ELM (genetic algorithm - extreme learning machine) model established by CARS (competitive adaptive reweighted sampling) method to optimise 12 chromaticity features of S chromaticity frequency sequence had the best prediction effect, with R_c of 0.917, R_p of 0.934 and residual predictive deviation (RPD) of 2.507. Therefore, the colour image information can accurately predict the moisture content of dried Hami jujube.

Keywords: chromaticity frequency sequence; colour mean; competitive adaptive reweighted sampling; extreme learning machine

Nowadays, *Zizyphus jujuba* Mill. (jujube fruit) has been much appreciated for its delicious taste and high nutritional value, hence an increasing number of people are planting jujube trees. Jujube fruit has been widely used as a crude drug and food for thousands of years (Li et al. 2005). Dried Hami jujubes are not only one of the most characteristic agricultural products in Xinjiang, but also an excellent nourishing food and medicinal food.

In recent years, computer vision (CV) has been widely used in the external quality detection and sorting of jujube fruit. Manickavasagan et al. (2014) determined the efficiency of RGB (red, green, blue) colour imaging technique to classify jujube fruits into three grades based on their hardness. Wu et al. (2016) proposed a hyperspectral imaging technique for acquiring

reflected images to identify common defects on the surface of jujube fruit. Dai et al. (2017) studied the image segmentation method of Lingwu long jujubes. A new extraction model of hue was proposed which improved the accuracy of extracting a jujube image. Luo et al. (2020) proposed a novel visual feature fusion based on connected region density, texture features, and colour features to evaluate the surface texture of dried Hami jujube. In comparison with other fusion methods, it has a better performance. However, most of these computer vision techniques have been applied to detect the external quality of jujube fruit (such as texture, size, and defect), while there is little literature on the internal quality of jujube fruit (such as moisture content).

Hami jujube has a short period of fresh food, and the water content of fresh jujube can be reduced to about

25%, which can effectively inhibit the growth of micro-organisms for storage and transportation (Zhao et al. 2014). Therefore, it is very important to determine the moisture content of Hami jujube rapidly and in a non-destructive way.

In recent years, image processing technology has been widely used in non-destructive detection of crop moisture, but few researchers have studied the water content of jujube fruits. The results of domestic and foreign studies show that the colour feature can be used as a non-destructive prediction index of crop water, and the relationship model between water content and mean colour is obtained. Ying et al. (2006) used computer vision technology to study citrus maturity, proposed the colour information method of describing the HSI (hue, saturation, intensity) colour space model of citrus image using the chromaticity frequency sequence method, and established the artificial neural network discrimination model, with the accuracy reaching 77.8%. Mohebbi et al. (2009) presented a method based on computer vision systems (CVS) to estimate the shrimp dehydration level by analysing colour during a drying process. Golpour et al. (2014) proved that the image analysis can be used to classify the rice cultivars by extracting 36 colour features in RGB, HSI, HSV (hue, saturation, value) spaces from the rice images. Barbedo (2016) proposed an algorithm combining H channel of HSV colour space and A channel of *Lab* colour space (*Lab*) to distinguish asymptomatic tissues and disease signs of plant leaves. Keskin et al. (2014) predicted the moisture content (MC) and nutrient content of peanut leaves from colour parameters (*CIELab*) using a chromameter. In order to explore the feasibility of colour feature information in predicting the moisture content of dried Hami jujube, the single-channel mean value and chromaticity frequency sequence of three colour space models of dried Hami jujube RGB, HSV and *CIELab* were extracted, and the prediction model of related moisture content was established by GA-ELM (genetic algorithm - extreme learning machine) algorithm. Furthermore, CARS (competitive adaptive reweighted sampling) was used to extract the features of the chromaticity frequency sequence of the extracted images to realise the rapid and non-destructive detection of the moisture content of dried Hami jujube.

MATERIAL AND METHODS

Image acquisition and moisture content measurement

Experimental material. The experimental material was dried Hami jujubes, purchased from the dried

fruit market in Hami City, Xinjiang, and 150 samples of uniform size without defects were selected as the experimental samples. After wiping the surface clean, number it and place it at room temperature [28~31 °C, 27~30% RH (relative humidity)] for 48 h to make the sample temperature consistent with the ambient temperature.

Image acquisition. In this experiment, images of dried jujube were acquired by a computer image acquisition system, which mainly consisted of an industrial camera (CV-M7+CL; Japan Analytical Industry Co., Ltd, Japan), collection box, LED strip light source (AFT-WL21244-22W, white light; Xi'an Weishi Company, China), computer (Intel® Core™ I7-8700 CPU @3.20GHz, Windows 10, Dell, USA), and image acquisition card (Guangzhou Yahui Precision Company, China). The stems of dried Hami jujubes were placed perpendicularly to the direction of the camera, the background colour was white. The distance between the lens and the object was 23.5 cm. The image acquisition system is shown in Figure 1.

Moisture content measurement. After the image acquisition is completed, the wet weight of the dry Hami jujube is measured and recorded using the electronic balance (JY/YP30002; Shanghai Leping Scientific Instruments Co., Ltd., China) with an accuracy of 0.0001 g. Then the fruit is put in the drying box (DHG-9070 A; Shanghai Yiheng Technology Co., Ltd, China), 220 V, 50 Hz, 1550 W, temperature control range: 10–250 °C for dehydration, drying temperature set to 105 °C, 4 h. Then continue to dry in the drying box for 0.5 h, repeat until the two front and rear weight errors do not exceed 0.002 g, that is, the constant weight of the sample, record the weight as the dry weight value of the sample at this time. The difference between wet weight and dry weight, divided by wet

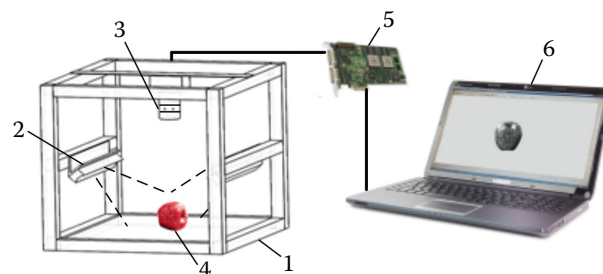


Figure 1. Schematic diagram of the image acquisition device

1 – collection box; 2 – LED (light-emitting diode) strip light source; 3 – industrial camera; 4 – dried Hami jujube; 5 – image acquisition card; 6 – computer

<https://doi.org/10.17221/109/2021-CJFS>

Table 1. Statistical analysis of moisture content of dried Hami jujube

Sample set	Moisture content				
	sample amount	maximum value (%)	minimum value (%)	average value (%)	SD (%)
Calibration set	100	0.2797	0.1070	0.1828	0.0351
Prediction set	50	0.2338	0.1301	0.1748	0.0280

SD – standard deviation

weight, calculates the moisture content of each sample. Table 1 shows the statistical results of the moisture content of 150 dry Hami samples divided into calibration sets and prediction sets.

Image processing

Image processing is to eliminate or suppress the effects of noise in order to highlight the characteristic information of the object under test. The images collected using industrial cameras in this article are $1030 \times 1380 \times 3$ pixels RGB images. These preprocessing treatments were performed using the MATLAB R2019b software (MathWorks, USA), details are as follows:

1) The RGB colour image was converted to a grayscale image, and the grayscale image was dimmed (threshold set to 0.5), and the pixel coordinates of the left, right, top, and bottom pixels in the Hami jujube image area (pixel value was 1) were calculated, so as to extract the colour image of the target ROI (region of interest) by means of the coordinates of the four points.

2) The R channel was extracted in the colour image, using the threshold segmentation method (threshold setting was 130), the image background was removed.

3) The morphological opening and closing operation with a radius of 3 pixels was carried out to remove the noise of burrs, holes and so on.

4) The target area hole was filled to form the target mask.

5) The target mask and the original image were multiplied to obtain the dried Hami jujube target.

6) The dried Hami jujube RGB colour space model was converted to HSV and *Lab* colour space models, respectively. See Figure 2.

Sample division

In this study, 150 Hami jujube samples were divided into calibration set (100) and prediction set (50) at the ratio of 2:1 by SPXY method (Galvao et al. 2005). The calibration set was applied to build the calibration model, and the prediction set was applied to assess the model performance. The sample division was calculated according to the following mathematical formulation (Equation 1):

$$d_{xy}(i, j) = \frac{d_x(i, j)}{\max_{i, j \in (1, z)} [d_x(i, j)]} + \frac{d_y(i, j)}{\max_{i, j \in (1, z)} [d_y(i, j)]} \quad (1)$$

where: $d_x(i, j)$ – the distance between colour characteristic samples; $d_y(i, j)$ – the distance between moisture content samples, and z – the number of samples. When dividing, d_x and d_y are divided by their respective maximum values, so that the x – y distance between each sample is obtained as the weight when selecting samples.

Image colour analysis

Colour mean values. The colour model component mean values are calculated by calculating the pixel

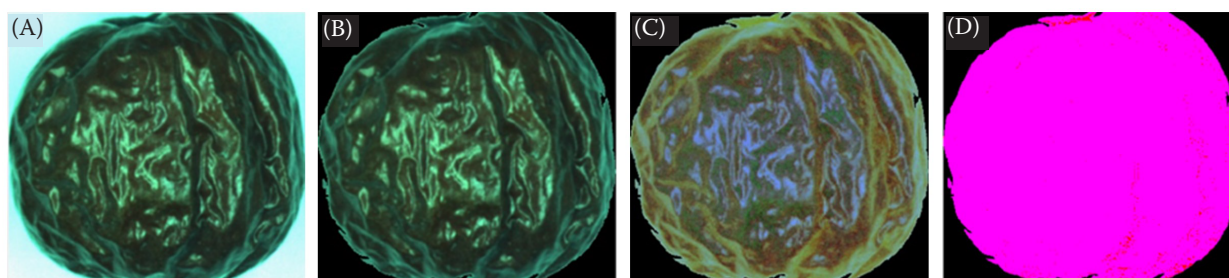


Figure 2. Result of the image processing of dried Hami jujube: (A) region of interest image, (B) background segmentation image, (C) image of HSV space model, (D) image of CIE Lab space model

HSV – hue, saturation, value

value of the pixels in the image and taking the average (Feng et al. 2020). After obtaining the three colour space model images of the 150 dried Hami jujube images after the background segmentation, the pixel values of the pixels in each chromaticity (R, G, B, H, S, V, L^* , a^* , b^*) were calculated and the average values were calculated. The colour model component mean values of 150 samples were obtained.

Chromaticity frequency sequence. Chromaticity frequency sequence is a method by counting the number of pixels corresponding to each chromaticity value in an image and then arranging it from low to high by colour value to describe the colour information of the image. Figure 3 is a statistical distribution of RGB colour space pixels after the background segmentation of the dry Hami jujube image. The horizontal coordinates in the figure are the chromaticity values of the colour. As can be seen from chromaticity theory, the colour value range of colours is (0, 1, 2, ..., 255). The ordinate coordinates in the figure correspond to the frequency of pixels corresponding to each chroma value in the image, which is the ratio of the number of pixels owned by each chromaticity in the image to the total number of pixels in the image.

Models and methods

Pearson correlation analysis was used to study the correlation of 9 colour model component mean values. In order to establish the dried Hami jujube

moisture evaluation model well, extreme learning machine (ELM) (Song et al. 2020), support vector regression (SVR) (Nikmaram et al. 2015), partial least squares regression (PLSR) (Kreeger 2013) were used for modelling analysis, and genetic algorithm (GA) was used for optimisation. In order to enhance the stability of ELM model, GA is used to optimise the connection weight between the input layer and the hidden layer and the neuron threshold of the hidden layer, so as to determine the optimal ELM model. Since the chromaticity frequency sequence extracted from each chromaticity of each dried Hami jujube image is a 256-dimensional vector, variable information that is highly related to the moisture content of the dried Hami jujube can be filtered out, thereby simplifying the model, and improving the operation of the model effectiveness. Here, CARS method (Huang et al. 2020; Yuan et al. 2020) is used to optimise the feature variables in the chrominance frequency sequence of 150 Hami jujube images.

Model performance assessment

The model performance was evaluated by the determination coefficient of calibration set (R_c), determination coefficient of prediction set (R_p), root mean square error of calibration set ($RMSEC$), root means the square error of prediction set ($RMSEP$), and root mean square error of cross validation ($RMSECV$). These evaluation indices have been defined elsewhere

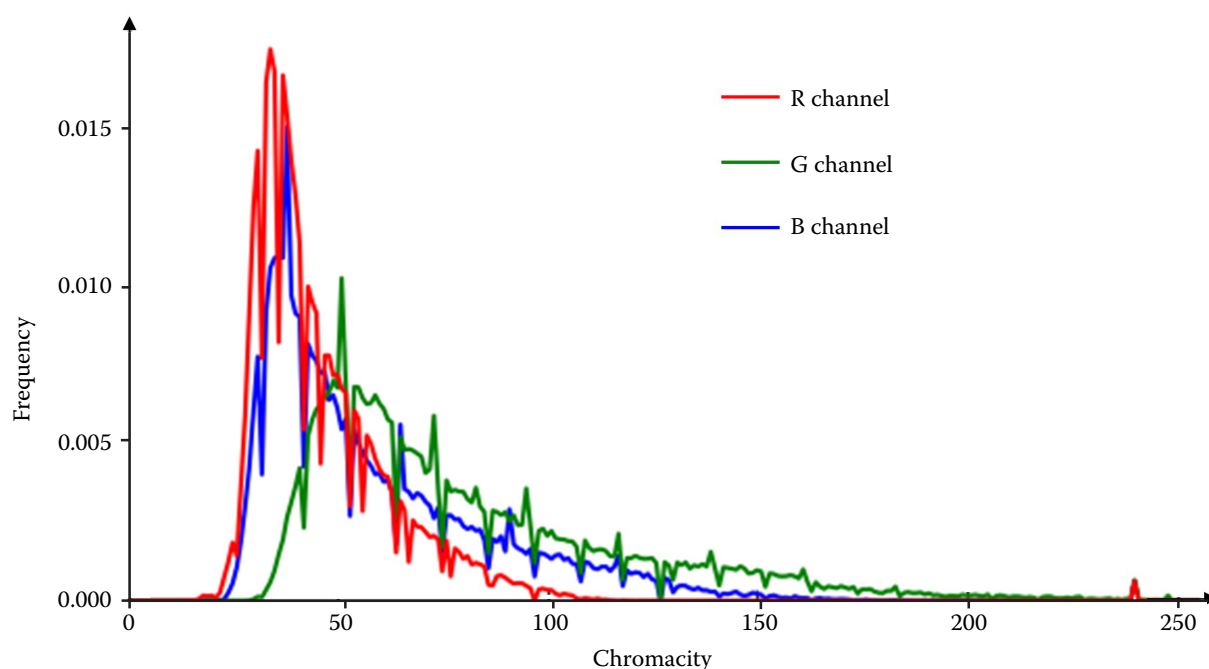


Figure 3. Chromaticity frequency sequence diagram of dried Hami jujube RGB colour space
RGB – (red, green, blue) colour imaging technique

<https://doi.org/10.17221/109/2021-CJFS>

(Guo et al. 2015). Besides, residual predictive deviation (*RPD*) was used to assess the predictive ability of a model. It is defined as follows (Equation 2):

$$RPD = SD_{\text{prediction}} / RMSEP \quad (2)$$

where: $SD_{\text{prediction}}$ – the standard deviation of the prediction set; $RMSEP$ – root mean square error of prediction set.

According to Nicolai et al. (2007), an *RPD* value less than 1.5 indicates very poor prediction, a value between 1.5 and 2.0 means that the model can discriminate low from high values of the response variable, a value between 2.0 and 2.5 indicates that coarse quantitative predictions are possible, and a value between 2.5 and 3.0 or above corresponds to good and excellent prediction accuracy.

RESULTS AND DISCUSSION

Model selection. Table 2 shows the results of three regression models for predicting the moisture content of dried Hami jujube. It was observed that the number of neurons in the hidden layer is equal while the R_p of ELM is slightly lower than that of PLSR, the R_c is much higher than that of PLSR. This shows that the ELM model is more suitable for predicting the moisture content of dried Hami jujube. After using the GA to optimise the ELM model, the prediction effect of the model has been greatly improved, with R_p of 0.841, *RPD* of 1.849.

Prediction model based on colour model component mean values. The Pearson correlation analysis method was used to analyse the correlation of 9 colour model components of R, G, B, H, S, V, L^* , a^* and b^* after image background segmentation, and the results are shown in Table 3.

It can be seen from Table 3 that, except for S colour model component, which has no correlation with water content, other colour model components are significantly correlated with moisture content. And it can be seen that the significance of G, S and L colour model

Table 2. Prediction results of moisture content model of dried Hami jujube

Model	<i>RMSEC</i>	<i>RMSEP</i>	R_c	R_p	<i>RPD</i>
ELM	0.012	0.011	0.824	0.825	1.767
PLSR	0.015	0.011	0.729	0.833	1.805
SVR	0.014	0.011	0.748	0.819	1.741
GA-ELM	0.011	0.011	0.872	0.841	1.849

ELM – extreme learning machine; PLSR – partial least squares regression; SVR – support vector regression; GA – genetic algorithm; *RMSEC* – root mean square error of calibration set; *RMSEP* – root mean square error of prediction set; R_c – determination coefficient of calibration set; R_p – determination coefficient of prediction set; *RPD* – residual predictive deviation

components is lower than the significance of the others. Therefore, we built moisture content prediction models of R, B, H, V, a^* and b^* colour model components and 9 colour model components.

We used GA-ELM to establish the model, select “sig” as the kernel function. The parameters of the GA were set as follows: the initial population was 50, the mutation probability was 0.005, the number of genetic iterations was 100, and the convergence rate was 0.5. The results of comparing the performance of the model with a different number of hidden layer neurons are shown in Table 4.

It can be seen that the number of hidden layer neurons had a great impact on the prediction ability and stability of the model, which had also been proved by Wu (2020). In addition, the prediction model based on 6 colour components was generally better than that based on 9 colour components, which indicated that screening colour components with no obvious correlation were beneficial for the model to better predict the moisture content of dried Hami jujube.

Prediction model based on chromaticity frequency sequence. The moisture content prediction models were established respectively through the chromaticity frequency sequence of 9 colour model components, and the optimal hidden layer of each model was selected

Table 3. Correlation analysis between moisture content and the mean value of each colour

Correlation coefficient	R	G	B	H	S	V	L^*	a^*	b^*
<i>R</i>	–0.68	0.39	0.74	–0.72	–0.09	0.71	–0.26	–0.74	–0.73
<i>P</i>	0	0	0	0	0.26	0	0	0	0

R, G, B, H, S, V, L^* , a^* , b^* – colour model component; *R* – correlation coefficient; (+) positive correlation; (–) negative correlation; *P* – significant coefficient; correlation has a significant difference at $P < 0.05$; correlation has an extremely significant difference at $P < 0.01$

Table 4. GA-ELM model prediction results of different colour components under different hidden layer neurons

Colour model component	Number of hidden layer neurons	$RMSEC$	$RMSEP$	R_c	R_p	RPD
R, G, B, H, S, V, L^* , a^* , b^*	35	0.012	0.010	0.832	0.868	2.013
	40	0.011	0.010	0.852	0.862	1.974
	45	0.011	0.010	0.857	0.855	1.928
	50	0.010	0.010	0.875	0.858	1.946
	55	0.010	0.011	0.887	0.830	1.793
	60	0.010	0.011	0.879	0.824	1.763
R, B, H, V, a^* , b^*	35	0.013	0.010	0.808	0.870	2.028
	40	0.012	0.009	0.840	0.885	2.144
	45	0.011	0.010	0.845	0.871	2.033
	50	0.010	0.009	0.875	0.887	2.162
	55	0.010	0.010	0.890	0.871	2.032
	60	0.009	0.011	0.895	0.828	1.785

R, G, B, H, S, V, L^* , a^* , b^* – colour model component; $RMSEC$ – root mean square error of calibration set; $RMSEP$ – root mean square error of prediction set; R_c – determination coefficient of calibration set; R_p – determination coefficient of prediction set; RPD – residual predictive deviation

through the model experiment. Table 5 shows the moisture content prediction results of chromaticity frequency sequence of different colour model components. It can be seen from Table 5 that the moisture content prediction performance of chromaticity frequency sequence of different colour model components was different, among which the moisture content prediction performance of the chromaticity frequency sequence of the H colour model component was the best when the hidden layer neuron is 40, which is only a little lower than the moisture content prediction model established by the 6 colour model components. Therefore, the model performance was improved by screening the charac-

teristic variables with high correlation with moisture content in the chromaticity frequency sequence.

Feature optimisation. In order to further simplify the model and improve the prediction performance of the model, CARS method was used to optimise the characteristic variables in the chromaticity frequency sequence of 9 colour model components. After the feature optimisation, GA-ELM is used to establish moisture content prediction models respectively. The number of hidden neurons setting was 50. The model results are shown in Table 6.

It can be seen from Table 6 that the performance of the moisture content prediction model of R, S, and V

Table 5. Moisture content prediction model of different chromaticity frequency sequences

Chromaticity frequency sequence	$RMSEC$	$RMSEP$	R_c	R_p	RPD
R	0.013	0.010	0.819	0.813	1.715
G	0.014	0.011	0.786	0.753	1.521
B	0.012	0.010	0.834	0.808	1.697
H	0.010	0.010	0.874	0.873	2.046
S	0.011	0.010	0.854	0.837	1.828
V	0.012	0.010	0.841	0.821	1.754
L^*	0.021	0.016	0.379	0.346	1.066
a^*	0.016	0.014	0.683	0.664	1.338
b^*	0.015	0.013	0.735	0.670	1.347

R, G, B, H, S, V, L^* , a^* , b^* – colour model component; $RMSEC$ – root mean square error of calibration set; $RMSEP$ – root mean square error of prediction set; R_c – determination coefficient of calibration set; R_p – determination coefficient of prediction set; RPD – residual predictive deviation

<https://doi.org/10.17221/109/2021-CJFS>

Table 6. Results of different chromaticity frequency sequences selected by CARS

Chromaticity frequency sequence	Feature number	$RMSEC$	$RMSEP$	R_c	R_p	RPD
R	9	0.011	0.008	0.847	0.913	2.446
G	22	0.008	0.014	0.937	0.673	1.352
B	26	0.011	0.010	0.861	0.833	1.810
H	40	0.011	0.010	0.871	0.841	1.849
S	12	0.011	0.007	0.917	0.934	2.507
V	31	0.010	0.009	0.899	0.871	2.038
L^*	2	0.021	0.016	0.379	0.350	1.066
a^*	10	0.012	0.014	0.844	0.583	1.231
b^*	23	0.014	0.014	0.763	0.566	1.213

CARS – competitive adaptive reweighted sampling; R, G, B, H, S, V, L^* , a^* , b^* – colour model component; $RMSEC$ – root mean square error of calibration set; $RMSEP$ – root mean square error of prediction set; R_c – determination coefficient of calibration set; R_p – determination coefficient of prediction set; RPD – residual predictive deviation

chromaticity frequency sequence was significantly improved after feature optimisation. Moreover, the moisture content prediction model of S chromaticity was the best, with R_c of 0.917, R_p of 0.934 and RPD of 2.507,

which was higher than six colour model components, indicating that CARS optimising features were more conducive to moisture content prediction. This was consistent with many previous studies (Hong et al. 2020;

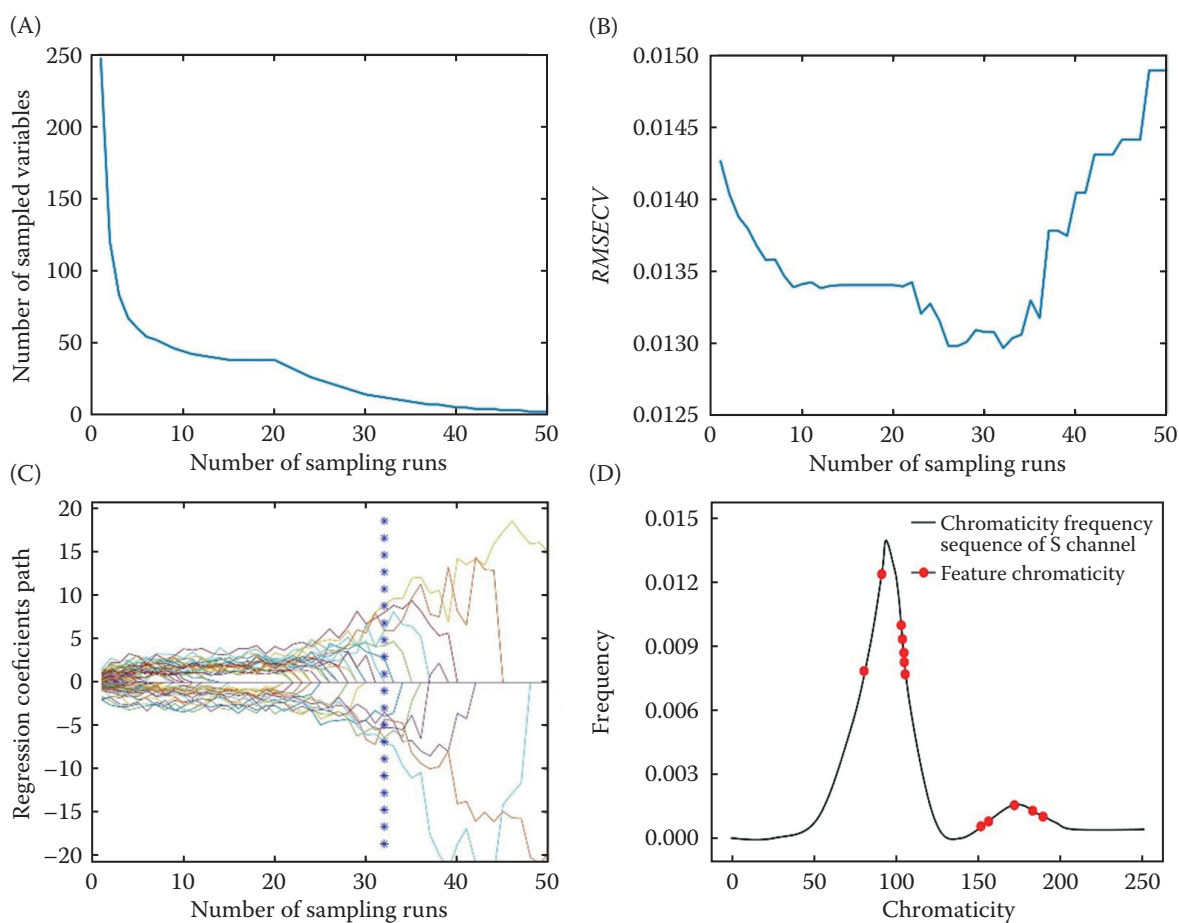


Figure 4. Feature optimisation process by CARS: (A) changes in the number of wavelength variables, (B) change in $RMSECV$, (C) variable regression coefficient trend, (D) distribution of feature chromaticity

CARS – competitive adaptive reweighted sampling; $RMSECV$ – root mean square error of cross validation

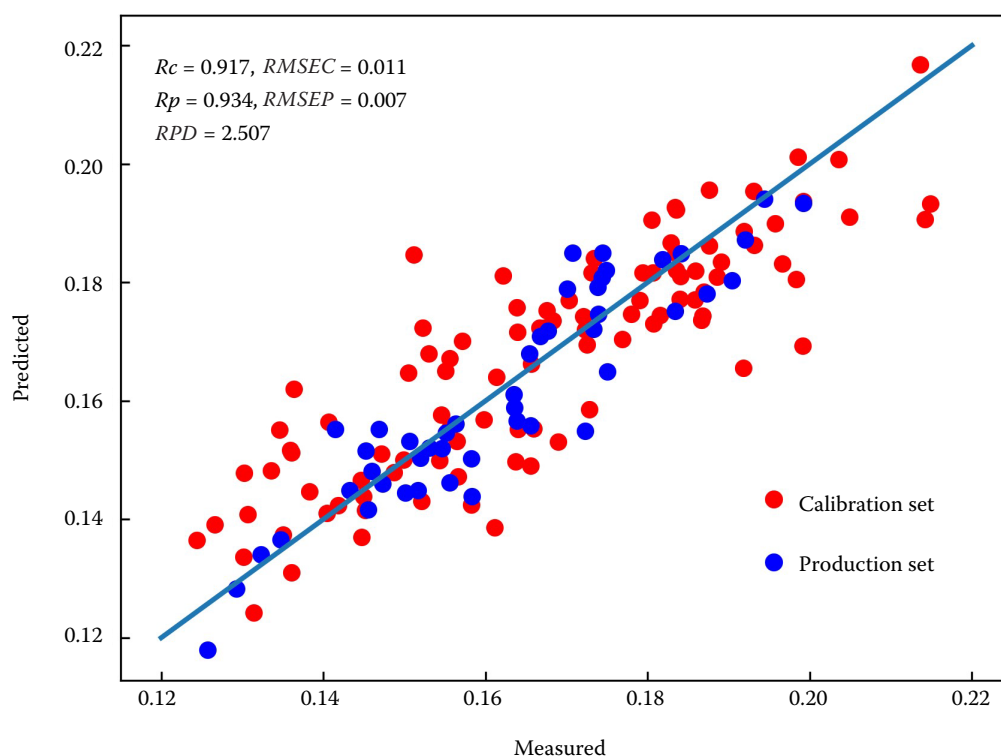


Figure 5. Scatter diagram between predicted and measured values of the calibration set and prediction set samples

R_c – determination coefficient of calibration set; R_p – determination coefficient of prediction set; $RMSEC$ – root mean square error of calibration set; $RMSEP$ – root mean square error of prediction set; RPD – residual predictive deviation

Shu et al. 2021). Figure 4 shows the feature optimisation process of chromaticity frequency sequence of S colour model components. Figure 5 shows the results of the moisture content model of dried Hami jujube established by 12 chromaticity features of S channel. It can be seen that the model established can better predict the moisture content of dried Hami jujube. Compared with reference Wang et al. (2020), the prediction result of the moisture prediction model of dried Hami jujube established in this paper was slightly lower, because the near-infrared spectrum can obtain more information of internal components, but in terms of the convenience of the method, this method was better.

CONCLUSION

The mean values and chromaticity frequency sequences of colours have a good correlation with the moisture content of dried Hami jujube. The GA-ELM model established after chromaticity optimisation can better predict the moisture content of dried Hami jujube. The results obtained demonstrated that image colour information can be used for non-destructive testing of the moisture content of dried Hami ju-

jube. In future research, in order to establish a more accurate and robust forecasting model, more samples from different years, of different origins and different varieties will be studied.

REFERENCES

- Barbedo J.G.A. (2016): A novel algorithm for semi-automatic segmentation of plant leaf disease symptoms using digital image processing. *Tropical Plant Pathology*, 41: 210–224.
- Dai Y.P., Wang Y.T., Xue J.R., Liu X.N., Liu B.H., Guo X.Y. (2017): Research of segmentation method on image of Lingwu Long Jujubes based on a new extraction model of Hue. *IEEE Sensors Journal*, 17: 6029–6036.
- Feng L., Li H.B., Gao Y.K., Zhang Y.K. (2020): A color image segmentation method based on region salient color and fuzzy c-means algorithm. *Circuits, Systems & Signal Processing*, 39: 586–610.
- Golpouri I., Parian J.A., Chayjan R.A. (2014): Identification and classification of bulk paddy, brown, and white rice cultivars with colour features extraction using image analysis and neural network. *Czech J. Food Sci.*, 32: 280–287.
- Guo W.C., Fang L.J., Liu D.Y., Wang Z.W. (2015): Determination of soluble solids content and firmness of pears during

<https://doi.org/10.17221/109/2021-CJFS>

- ripening by using dielectric spectroscopy. *Computers and Electronics in Agriculture*, 117: 226–233.
- Galvao R.K.H., Araujo M.C.U., Jose G.E., Pontes M.J.C., Silva E.C., Saldanha T.C.B. (2005): A method for calibration and validation subset partitioning. *Talanta*, 67: 736–740.
- Huang Y.F., Dong W.T., Sanaeifar A., Wang X.M., Luo W., Zhan B.S., Liu X.M., Li R.L., Zhang H.L., Li X.L. (2020): Development of simple identification models for four main catechins and caffeine in fresh green tea leaf based on visible and near-infrared spectroscopy. *Computers and Electronics in Agriculture*, 173: 1–8.
- Hong Y.S., Chen S.C., Chen Y.Y. (2020): Comparing laboratory and airborne hyperspectral data for the estimation and mapping of topsoil organic carbon: Feature selection coupled with random forest. *Soil and Tillage Research*, 199: 1–14.
- Keskin M., Karanlik S., Keskin S.G., Soysal Y. (2014): Utilization of color parameters to estimate moisture content and nutrient levels of peanut leaves. *Turkish Journal of Agriculture and Forestry*, 37: 604–612.
- Kreeger P.K. (2013): Using partial least squares regression to analyze cellular response data. *Science Signaling*, 6: 1–5.
- Li J.W., Ding S.D., Ding X.L. (2005): Comparison of antioxidant capacities of extracts from five cultivars of Chinese jujube. *Process Biochemistry*, 40: 3607–3613.
- Luo X.Z., Ma B.X., Wang W.X., Lei S.Y., Hu Y.Y., Yu G.W., Li X.Z. (2020): Evaluation of surface texture of dried Hami Jujube using optimised support vector machine based on visual features fusion. *Food Science and Biotechnology*, 29: 493–502.
- Manickavasagan A., Al-Mezeini N.K., Al-Shekaili H.N. (2014): RGB color imaging technique for grading of dates. *Scientia Horticulturae*, 175: 87–94.
- Mohebbi M., Akbarzadeh M.R., Shahidi F., Moussavi M., Ghodusi H.B. (2009): Computer vision systems (CVS) for moisture content estimation in dehydrated shrimp. *Computers and Electronics in Agriculture*, 69: 128–134.
- Nikmaram P., Mousavi S., Emam-Djomeh Z., Kiani H., Razavi S. (2015): Evaluation and prediction of metabolite production, antioxidant activities, and survival of *Lactobacillus casei* 431 in a pomegranate juice supplemented yogurt drink using support vector regression. *Food Science and Biotechnology*, 24: 2105–2112.
- Nicolai B.M., Beullens K., Bobelyn E., Peirs A., Saeys W., Theron K.I., Lammertyn J. (2007): Non-destructive measurement of fruit and vegetable quality by means of NIR spectroscopy: A review. *Postharvest Biology and Technology*, 46: 99–118.
- Song G., Dai Q., Han X.M., Guo L. (2020): Two novel ELM-based stacking deep models focused on image recognition. *Applied Intelligence*, 50: 1345–1366.
- Shu M.Y., Shen M.Y., Zuo J.Y., Yin P.F., Ma Y.T. (2021): The application of UAV-based hyperspectral imaging to estimate crop traits in maize inbred lines. *Plant Phenomics*, 2021: 1–12.
- Wang W.X., Ma B.X., Luo X.Z., Li X.X., Lei S.Y., LI Y.J., SUN J.T. (2020): Study on moisture content of dried Hami big jujubes by near-infrared spectroscopy combined with variable preferred and GA-ELM model. *Spectroscopy and Spectral Analysis*, 40: 543–549.
- Wu L.G., He J.G., Liu G.S., Wang S.L., He X.G. (2016): Detection of common defects on jujube using Vis-NIR and NIR hyperspectral imaging. *Postharvest Biology and Technology*, 112: 134–142.
- Wu C.D. (2020): Classification of catenary equipment based on a coupled genetic algorithm-extreme learning machine method. *Insight*, 62: 15–21.
- Ying Y.B., Xu H.R., Xu Z.G. (2006): Non-destructive maturity evaluation of citrus by hue frequency sequence method. *Journal of Biomathematics*, 21: 306–312.
- Yuan L.M., Mao F., Huang G.Z., Chen X.J., Wu D., Li S.J., Zhou X.Q., Jiang Q.J., Lin D.P., He R. (2020): Models fused with successive CARS-PLS for measurement of the soluble solids content of Chinese bayberry by vis-NIRS technology. *Postharvest Biology and Technology*, 169: 1–9.
- Zhao H.X., Zhang H.S., Li Q., Xu S. (2014): Research progress of drying technology of jujube. *Science and Technology of Food Industry*, 35: 379–382.

Received: May 11, 2021

Accepted: December 8, 2021

Published online: February 18, 2022